Applied Mathematics & Information Sciences
*An International Journal*

http://dx.doi.org/10.18576/amis/180310

# Prediction of Damping Ratio and Shear Modulus of Saturated Clay Soil under Rotating Machine

*Mohammed Y. Fattah*[1,*], *Ahmed S. Abdulrasool*[1], *Mohamed A. Hafez*[2], *Nahla M. Salim*[1], *and Anna R. Haroon*[2]

[1]Civil Engineering Department, University of Technology, Baghdad, Iraq
[2]Department of Civil Engineering, Faculty of Engineering, FEQS, INTI -IU Universi, Nilai -Malaysia

Received: 10 Oct. 2023, Revised: 2 Dec. 2023, Accepted: 20 Mar. 2024
Published online: 1 May 2024

**Abstract:** Developing countries' industrial growth necessitates innovative machine foundation design and resilient infrastructure. Meanwhile, soil properties play a significant role in the satisfactory design of machine foundations. The paper presents an experimental work to determine accurately the damping ratio and shear modulus by equations. The paper studies the effect of different parameters (embedded depth of foundation, shape of footing, and changing operating frequency of machine) on the damping ratio and shear modulus of saturated clay soil. Moreover, mathematical expressions are derived from statistical analysis to predict the damping ratio for rectangular and circular footing on saturated clay. The physical model results reveal that the damping ratio inside the soil will be increased with an increase in the depth of the point inside the soil for all cases. The damping ratio tends to decrease with an increase in operating frequency. The maximum damping ratio has occurred below a rectangular foundation with a 16.6 Hz operating frequency in saturated clay. The damping ratio is a function of many factors, such as embedment depth, degree of saturation, shape of foundation, and operation frequency of the machine.

**Keywords:** Damping ratio; shear modulus; machine foundation; clay soil.

## 1 Introduction

The soil system is complex; however, correctly evaluating dynamic soil properties is the most difficult task. These properties may vary from site to site, location to location, and machine to machine, as well as with variations in foundation depth. Under the influence of dynamic forces, the foundation interacts with the soil, activating dynamic soil-structure interaction and significantly influencing the dynamic response of the machine foundation system [1].

The shear modulus, elastic modulus, mass density, coefficient of subgrade reaction, and damping ratio of the soil must be known for the design of machine foundations subjected to vibration, calculation of ground response during an earthquake, analysis of the stability of slopes during an earthquake, and other dynamic analysis of soil. Shear modulus and damping ratio are considered more reliable parameters [2].

The number of loading cycles has been correlated to a decrease in shear modulus with an associated pore pressure increase, as summarized by [3]. The over-consolidation ratio and plasticity index are also influential in clay behavior.

Damping is an inherent property of soil, and its influence on forced vibration response is significant but during resonance or near resonance conditions. Different soils exhibit different damping properties depending on their composition and other characteristics. In the case of embedded foundations, the embedment depth also influences the damping properties [4].

The damping behavior of soils is also influenced by effective confining pressure. Influence of parameters such as confining pressure, void ratio, geologic age, cementation, etc. [5].

The shear strains developed in the supporting soil medium caused by the dynamic loading from machine foundations are usually much smaller than those produced by static loading. The value of the soil shear modulus at smaller strains (Gmax) is much higher than its corresponding value at larger strains [1].

Most of the investigations studied the damping ratio by resonant column test, but this test does not represent the actual state because it cannot represent the soil-structure interaction and geometrical damping.

[6] studied the dynamic characteristics of reconstituted and undisturbed cohesive soils utilizing resonant-column tests. Results showed the influence of various soil parameters, such as confining stress, over-consolidation ratio, void ratio, plasticity index, calcium carbonate content, and time of confinement on shear modulus and damping ratio at small and high shear strains are presented. Researchers found the damping ratio increases at high strains over its small-strain value.

[7] investigated the effect of clay saturation on soil's dynamic properties, including shear modulus (G) and

*Corresponding author e-mail: 40011@uotechnology.edu.iq

damping ratio (D), by resonant column tests. The Poisson's ratio (ν) of the compacted clays was also determined. The samples measuring 50 mm × 100 mm were prepared in a constant volume mold at optimum moisture content under a static compaction. The first series samples were compacted at optimum moisture content, while the second series samples were fully saturated. The result indicated reduced shear modulus and increased damping ratio with saturation.

[8] and [9] carried out an experimental study on the behavior of dry, dense sand under the action of a single impulsive load. Emphasis was made on attenuation of waves induced by impact loads through the soil. The research also includes studying the effect of footing embedment and footing area on soil behavior and its dynamic response. Different falling masses from different heights were conducted using the falling weight deflectometer (FWD) to provide the single pulse energy. The responses of different soils were evaluated at different locations (vertically below the impact plate and horizontally away from it). It was concluded that increasing the footing embedment depth increases the amplitude of the force-time history by about 10-30% due to the degree of confinement increase. But, when embedding a footing, the surrounding soil restricts oscillation due to confinement, increasing the natural frequency. Increasing the footing embedment depth increases the damping ratio by about 50-150%.

[10] used many models to predict the dynamic behavior of soil (shear modulus and material damping). Two universal mathematical models were proposed to predict the normalized shear modulus reduction and material damping curves. The results indicated that the proposed model forms can accurately model the dynamic soil properties within the typical earthquake range.

This paper presents the results of a small-scale physical model to evaluate the damping ratio and shear modulus of clay soil under dynamic vertical load.

## 2 Physical Model and Soil Used

The soil tested in this paper is obtained from the Al-Rashid camp embankment. The specific gravity is 2.67, and the grain size distribution for the clay soil is found by ASTM D422, 2007 (3% sand, 38% silt, 59% clay) as shown in Fig. 1. Following the ASTM D4318, 2007, the Atterberg limits are 24% plasticity index, 23% plastic limit, and the liquid limit is 47%. It may be noted that based on the plasticity characteristics, the soil would be classified as CL using the Unified Soil Classification System.

After some trial testing, the clay soil was prepared at 20 kPa undrained shear strength to find a relationship between the undrained shear strength and water content, as shown in Fig. 2.

Numerical analysis by finite element was used to get the dimensions of the container test (720 x 720 x 560 mm) as proposed by [11]. The absorbing layer was positioned at the container's edge and bottom to simulate the soil's semi-infinite extension.

Two types of foundations, 100 mm diameter and 100x200 mm dimensions (circular and rectangle), are used. They are positioned on the soil surface and embedment depths (0.5 B and B). A rotating machine applies the vertical harmonic vibration to the middle of the foundations. The clay soil was placed in eight layers. Each layer was compacted by a timber rod to remove the air. Two water content sensors were used in the top and middle of the soil in the container box to ensure a uniform distribution of water content before the test, as shown in Fig. 3.

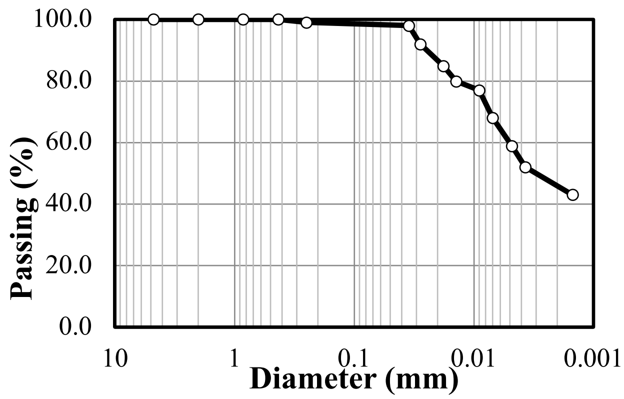


**Fig. 1**:Grain size distribution of the clay soil.

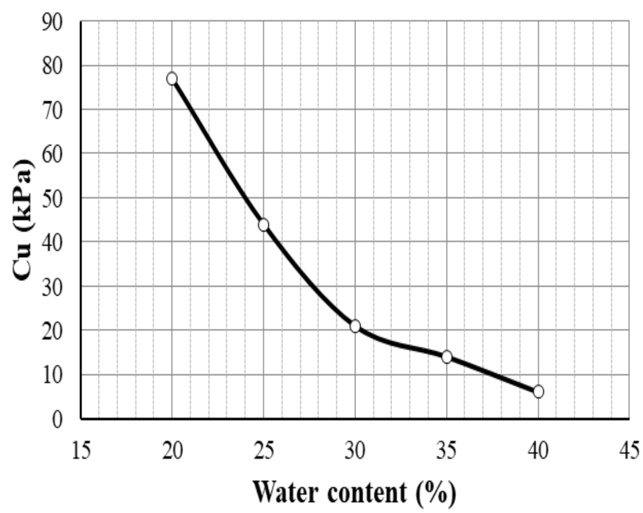


**Fig. 2.** Variation of the undrained shear strength with water content for the remolded clay after 48 hours of curing.

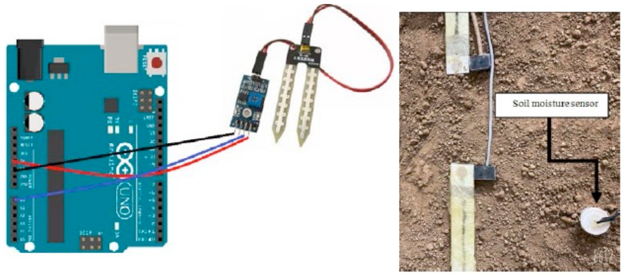


**Fig. 3:** The soil moisture sensor with Arduino data logger.

A small-scale oscillator was produced for testing the model in the laboratory atmosphere. Also, such equipment is named a 2-mass oscillator. The required equipment for inducing vibration comprises (2) AC motors working together but revolving in conflicting directions. Every motor comprises a power of 400 watts, an electric potential of 240 volts, and an alternating current motor speed controller (speed range 0–4500 rpm). Via changing the voltage delivered to the motor with the aid of the control unit of speed, the motor and oscillator speed can be changed, which, in sequence, results in a variation within the frequency of vibration created via the oscillator. A mechanical assemblage is fixed on the disc of the oscillator connected to a tachometer to measure the system's frequency. An eccentric weight

14.71 g has been placed as a rotating disk with a diameter of 75 mm and a thickness of 11 mm. This weight is positioned at an eccentricity distance, eo of 27.5 mm from the rotation axis. The force horizontal component abandons the equivalent eccentric weight component upon the other motor and the other manner about. Only the vertical force portion is remaining [12].

The amplitude harmonic vibrating force (Fo) can be found in the vertical positions by:

$$F_o = 2\, m_e\, e_o \omega^2 \quad (1)$$

where ω = angular frequency of each counter-rotating machine, I refer to eccentricity mass, and so is an eccentricity distance. The mechanical oscillator produces a sinusoidal harmonic vibration; the vertical vibrating force of all times can be represented as:

$$F(t) = F_o \sin \omega\, t \quad (2)$$

Details of the main features of the inducing vibration (actuator) and soil in the container test are shown in Fig. 4.

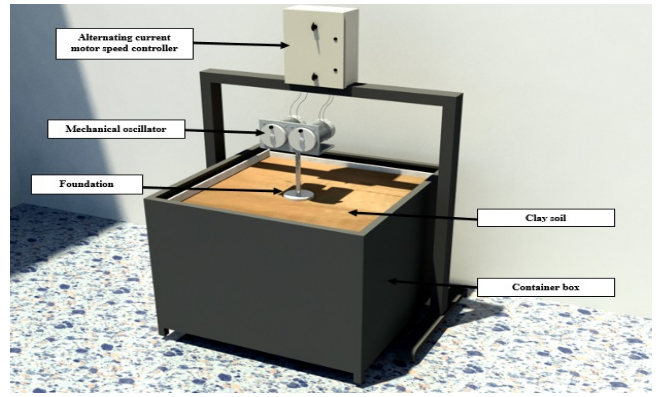


**Fig. 4:** Equipment for inducing vibration and soil in the test container.

## 3 A Proposed Methodology

### *3.1 Description of Problem*

Consider an elastic saturated clay soil subjected to vertical harmonic vibration. The natural circular frequency ($\omega_n$) of the foundation-soil system can be estimated by using the theory of vibration according to [13] and [14].

$$\omega_n = \sqrt{\frac{K}{m+m_s}} \quad (3)$$

where K is the soil spring constant (N/m), and m is the total mass of the foundation (kg). ms- the mass of the soil participating in vibration (kg).

A general guideline is to choose this value to be ranging between zero and the magnitude of the machine's mass and foundation [15].

In this study, the mass of the soil participating in the vibration is equal to that of the sensor receiving the vibration at different depths below the foundation.

The soil modulus of elasticity is estimated according to [16] using Eq. 4 and Eq. 5:

$$\omega_n = \sqrt{\frac{C_e\, A}{m_t}} \quad (4)$$

$$C_e = \frac{\alpha\, E}{(1-\upsilon^2)} \frac{1}{\sqrt{A}} \quad (5)$$

The α is considered equal to 1.09, as recommended by [15]. The soil spring constant (K) is measured directly by dividing the load measured inside the soil by the displacement based on the following equation.

$$K = \frac{P}{S} \quad (6)$$

where K is the soil spring constant (N/m), P is the load inside the soil (N), and S is displacement inside the soil (m).

Fig. 5 shows the soil spring constant under an operating frequency of (16.6 Hz) at different depths of sensors.

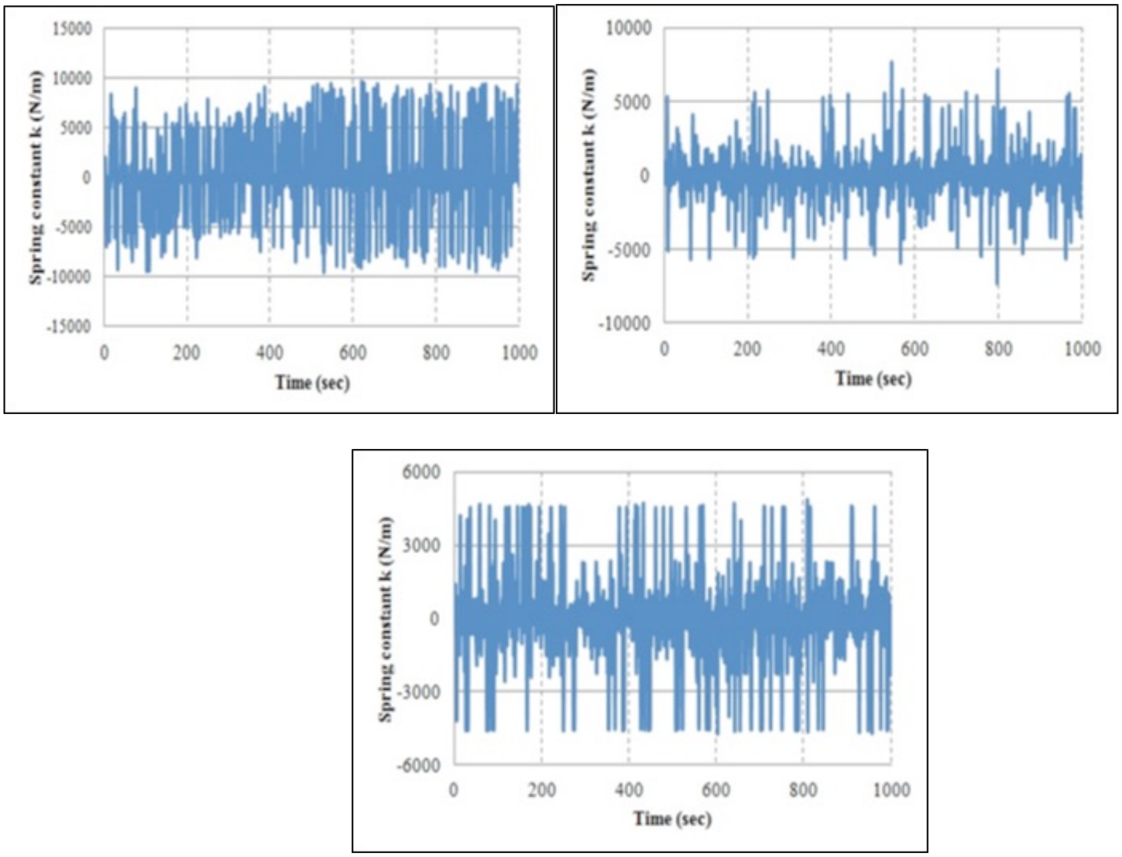


**Fig.5:** Variation for the soil spring constant under an operating frequency of (16.6 Hz) in a circular foundation on the surface of soft clay at different depths of sensors :(a) 0.5 B; (b) B; (c) 2B.

For isotropic material, the shear modulus, G, can be calculated using the following equation [17]:

$$G = \frac{E}{2(1+\upsilon)} \quad (7)$$

The equation of motion for a single degree of freedom system, as shown in Fig. 6, can be given as:

$$m_t\,\ddot{u} + c\,\dot{u} + k\,u = F(t) \quad (8)$$

Where ( $\ddot{u}$ ) is the acceleration, $\dot{u}$ is the velocity, u is the displacement, mt is the equivalent soil mass and foundation (kg), c is damping coefficient ((N Sec)/m), K is the spring constant ((N)/m), and F(t) is force (N).

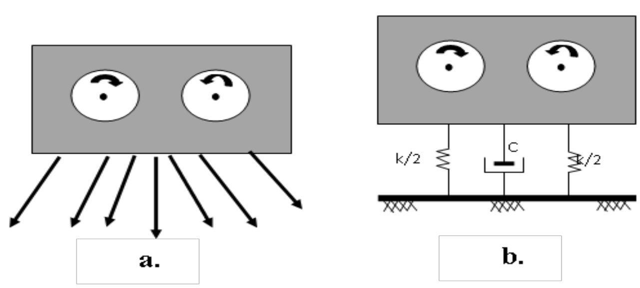


**Fig. 6:** A lumped parameter vibrating system [18].

This research uses equation (8) to find the damping coefficient. The damping ratio is a dimensionless parameter describing how an oscillating or vibrating body rests. Modeling the damping, which represents the percentage of energy loss per vibration cycle, is also extremely important both in structural design and in several seismological relations, but it remains one of the most complex issues.

A sinusoidal harmonic vibration was applied as a half-sine wave for the case under consideration. Accordingly, the damping ratio may be defined alternatively as the energy lost per cycle divided by the critical damping coefficient and evaluated as follows:

$$D = \frac{1}{\pi}\frac{c}{c_c} \quad (9)$$

It is important to say that the damping ratio in eq. (9) is calculated for one cycle, and only the positive part of the sinusoidal wave is considered.

$$c_c = 2\omega_n\, m_t \quad (10)$$

where: $c_c$ is the critical damping coefficient $\left(\frac{\text{N Sec}}{\text{m}}\right)$, $\omega_n$ is the natural circular frequency (rad/sec), and $m_t$ is the equivalent soil and foundation mass (kg).

This method is suggested to solve the problem and calculate the damping ratio.

## 4 Results of Soil Characteristics for Saturated Clay under Vertical Harmonic Vibration

A procedure is developed to evaluate the soil stiffness and damping ratio. Accordingly, the obtained values of spring constant, elastic and shear modulus, and damping ratios for different soils and harmonic vibration load conditions in saturated clay soil are listed in Tables 1 and 2. Figs. 7 to 12 presents the variation of damping ratio and shear modulus with depth in saturated clay soil.

These results show the effect of operating frequency on the shear modulus for all tests. The soil damping ratio, D, increases with embedded depth for all tests.

**Table 1.** Summary of saturated clay soil characteristics below a circular foundation with different operating frequencies.

| | Operating frequency (Hz) | Sensor No. | K N\m (eq. 7.5) | E $N/m^2$ (eq. 7.4) | G $N/m^2$ (eq. 7.7) | C N. Sec/m (eq. 7.8) | D % (eq. 7.10) |
|---|---|---|---|---|---|---|---|
| Circular foundation on surface | 16.6 | 1 | 9427 | 58003.2 | 19334.4 | 4.26 | 4 |
| | | 2 | 7686 | 47290.4 | 15763.4 | 6.98 | 7.3 |
| | | 3 | 4660 | 28675.6 | 9558.5 | 17.66 | 23.7 |
| | 33.3 | 1 | 12611 | 77598.4 | 25866.1 | 3.89 | 3.1 |
| | | 2 | 10056 | 61873.9 | 20624.6 | 5.87 | 5.3 |
| | | 3 | 7045 | 43339.9 | 14446.6 | 10.94 | 11.9 |
| | 50 | 1 | 22188 | 136551.9 | 45517.3 | 4.08 | 2.5 |
| | | 2 | 19454 | 119703.9 | 39901.3 | 5.98 | 3.9 |
| | | 3 | 15559 | 95738.5 | 31912.8 | 9.01 | 6.6 |
| Circular foundation at embedment depth 0.5 B | 16.6 | 1 | 10131 | 62345.1 | 20781.7 | 4.90 | 4.4 |
| | | 2 | 8311 | 51140.8 | 17046.9 | 7.49 | 7.5 |
| | | 3 | 5214 | 32074.2 | 10691.4 | 19.19 | 24.4 |
| | 33.3 | 1 | 13852 | 85247.1 | 28415.7 | 4.13 | 3.2 |
| | | 2 | 11213 | 68993.7 | 22997.9 | 6.44 | 5.5 |
| | | 3 | 8132 | 50039.0 | 16679.6 | 13.04 | 13.2 |
| | 50 | 1 | 23419 | 144116.6 | 48038.8 | 4.34 | 2.6 |
| | | 2 | 20529 | 126334.5 | 42111.5 | 6.26 | 4 |
| | | 3 | 16742 | 103024.9 | 34341.6 | 9.80 | 6.9 |
| Circular foundation at embedment depth B | 16.6 | 1 | 11139 | 68543.0 | 22847.6 | 5.14 | 4.5 |
| | | 2 | 9185 | 56522.6 | 18840.8 | 8.28 | 7.9 |
| | | 3 | 5924 | 36446.3 | 12148.7 | 26.00 | 31 |
| | 33.3 | 1 | 15578 | 95871.4 | 31957.1 | 4.60 | 3.3 |
| | | 2 | 12751 | 78462.6 | 26154.2 | 7.41 | 6 |
| | | 5 | 6687 | 41149.9 | 13716.6 | 60.19 | 67.6 |
| | 50 | 1 | 25470 | 156746.3 | 52248.7 | 5.37 | 3 |
| | | 2 | 22302 | 137251.4 | 45750.4 | 7.30 | 4.4 |
| | | 3 | 18477 | 113686.3 | 37895.4 | 11.47 | 7.7 |

**Table 2.** Summary of saturated clay soil characteristics below a rectangular foundation with different operating frequencies.

| | Operating frequency (Hz) | Sensor No. | K N\m (eq. 7.5) | E N/m² (eq. 7.4) | G N/m² (eq. 7.7) | C N. Sec/m (eq. 7.8) | D % (eq. 7.10) |
|---|---|---|---|---|---|---|---|
| **Rectangular foundation on the surface** | 16.6 | 1 | 9017 | 55485.4 | 18495.1 | 4.67 | 4.5 |
| | | 2 | 7263 | 44692.1 | 14897.3 | 7.54 | 8.1 |
| | | 3 | 4177 | 25701.0 | 8567.0 | 21.41 | 30.4 |
| | 33.3 | 1 | 11827 | 72768.5 | 24256.1 | 4.22 | 3.5 |
| | | 2 | 9886 | 60830.9 | 20276.9 | 6.72 | 6.2 |
| | | 3 | 6851 | 42149.5 | 14049.8 | 13.19 | 14.6 |
| | 50 | 1 | 21732 | 133740.2 | 44580.0 | 4.19 | 2.6 |
| | | 2 | 18714 | 115168.9 | 38389.6 | 7.08 | 4.7 |
| | | 3 | 14677 | 90313.4 | 30104.4 | 10.86 | 8.2 |
| **Rectangular foundation at embedment depth 0.5 B** | 16.6 | 1 | 9623 | 59209.8 | 19736.6 | 5.38 | 5 |
| | | 2 | 7847 | 48286.1 | 16095.3 | 8.91 | 9.2 |
| | | 3 | 4722 | 29055.3 | 9685.1 | 23.49 | 31.4 |
| | 33.3 | 1 | 13852 | 85247.1 | 28415.7 | 4.61 | 3.6 |
| | | 2 | 10013 | 61617.7 | 20539.2 | 7.62 | 7 |
| | | 3 | 7132 | 43878.3 | 14626.1 | 15.49 | 16.8 |
| | 50 | 1 | 22119 | 136107.7 | 45369.2 | 5.09 | 3.1 |
| | | 2 | 20529 | 126334.5 | 42111.5 | 9.76 | 6.2 |
| | | 3 | 16742 | 103024.9 | 34341.6 | 12.69 | 9 |
| **Rectangular foundation at embedment depth B** | 16.6 | 1 | 10566 | 65012.3 | 21670.7 | 6.40 | 5.7 |
| | | 2 | 8698 | 53519.3 | 17839.7 | 9.66 | 9.5 |
| | | 3 | 5323 | 32755.0 | 10918.3 | 29.19 | 36.7 |
| | 33.3 | 1 | 14362 | 88386.8 | 29462.2 | 5.14 | 3.9 |
| | | 2 | 10880 | 66954.9 | 22318.3 | 10.17 | 8.9 |
| | | 3 | 7648 | 47066.4 | 15688.8 | 26.68 | 28 |
| | 50 | 1 | 23280 | 143269.6 | 47756.5 | 5.74 | 3.4 |
| | | 2 | 21042 | 129469.3 | 43156.4 | 11.06 | 7 |
| | | 3 | 17359 | 106810.4 | 35603.4 | 16.03 | 11.1 |

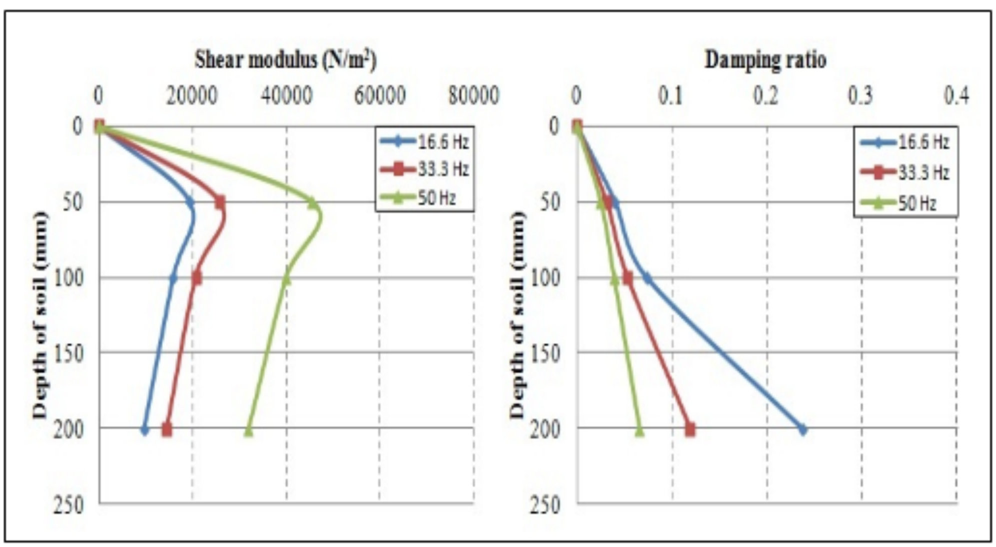


**Fig. 7:** Measured shear modulus and damping ratio with a depth of saturated clay soil for the circular foundation on the surface with different operating frequencies at points in the centerline under the foundation.

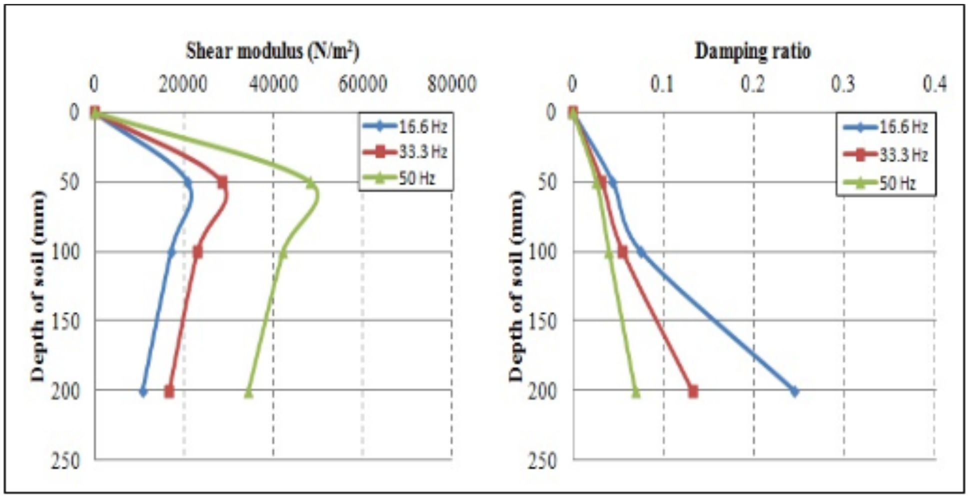


**Fig. 8:** Measured shear modulus and damping ratio with a depth of saturated clay soil for the circular foundation on embedment depth 0.5B with different operating frequencies at points in the centerline under the foundation.

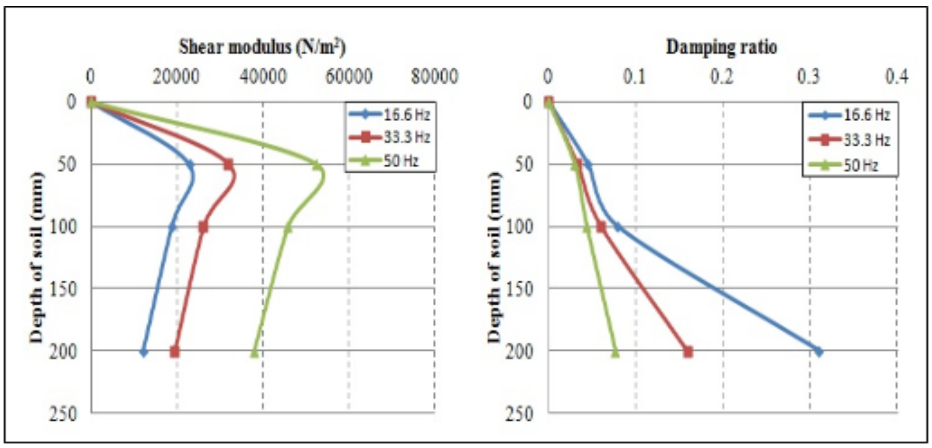


**Fig. 9:** Measured shear modulus and damping ratio with a depth of saturated clay soil for the circular foundation on embedment depth B with different operating frequencies at points in the centerline under the foundation.

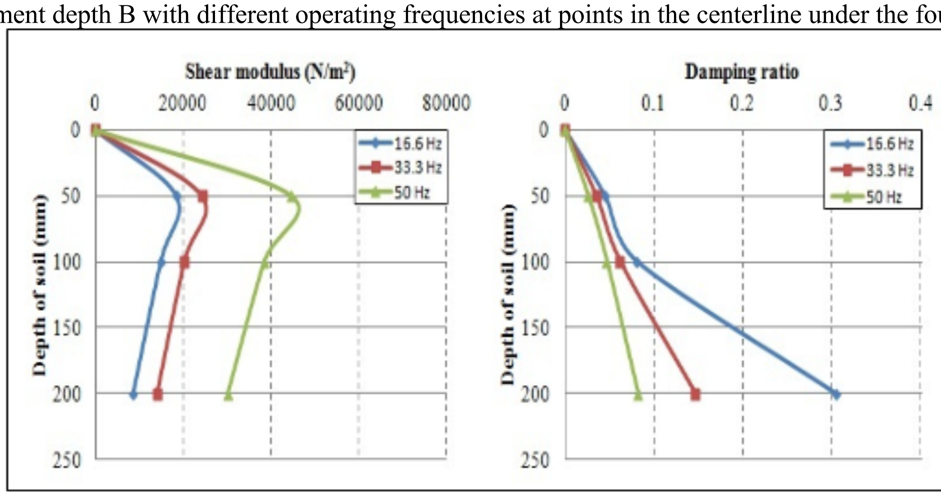


**Fig.10:**Measured shear modulus and damping ratio with a depth of saturated clay soil for a rectangular foundation on the surface with different operating frequencies at points in the centerline under the foundation.

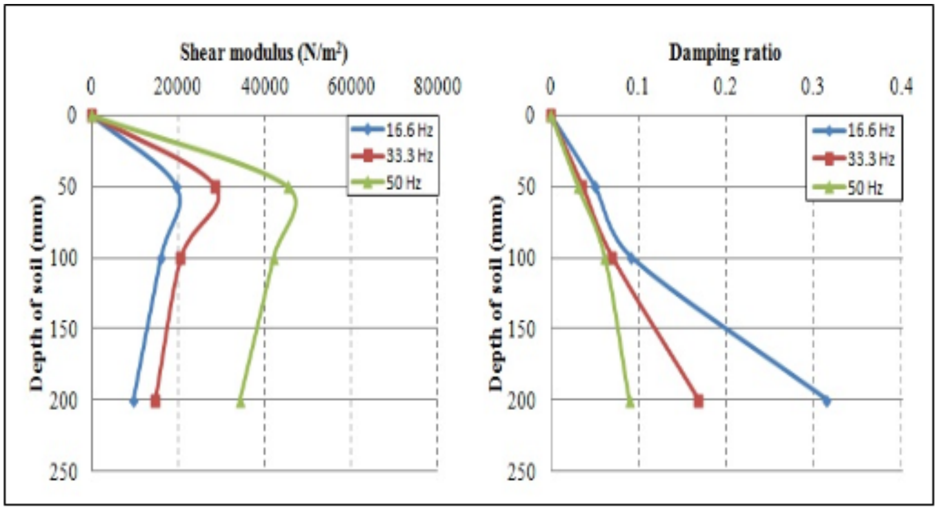


**Fig. 11:** Measured shear modulus and damping ratio with the depth of saturated clay soil for the rectangular foundation on embedment depth 0.5B with different operating frequencies at points in the centerline under the foundation.

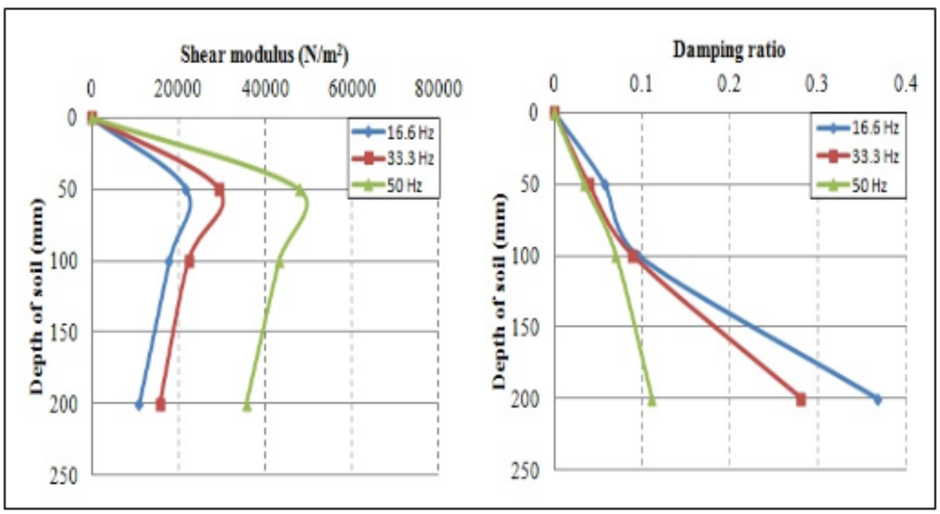


**Fig. 12**. Measured shear modulus and damping ratio with the depth of saturated clay soil for the rectangular foundation on embedment depth B with different operating frequencies at points in the centerline under the foundation.

From Figs. 7 to 12, the damping ratio increases with the depth of soil due to the dissipation of waves, which is related to frictional behavior at contacts. However, the reversible behavior between the damping ratio and shear modulus should be noted. This is due to the possibility that the elevation of the confining pressure plays an important role in energy dissipation during the dynamic excitation, and shear stress is decreased with increased soil depth.

The Young's modulus and shear modulus increase with increasing the total stress level. That is because of the progressive hardening induced by the vertical stress; the same data highlights that an increase in the number of cycles leads to a reduction of damping because of the sample hardening. These results coincide with the findings of [19]. The shear modulus and modulus of elasticity have functioned to the magnitude of the foundation's dynamic load, depth, and size.

Attenuation on soils is commonly estimated from the spatial decay of Rayleigh or Love waves by recording the ground motion at different distances from an active source.

According to the results, the damping ratio is adopted to find the mathematical expression—the mathematically modeled in the form of the most suitable equations derived using the SPSS software.

Two equations are adopted with different variables. The required equation should represent the best prediction of the damping ratio inside the soil depending on the degree of saturation, operating frequency, embedment depth of the foundation, and point location.

- Circular foundation on saturated soil:

D = – 6.573 – 0.107×Freq + 0.031×Emb. + 0.109×Cent. + 0.386×Bes. (11)

- Rectangular foundation on saturated soil:

D = – 8.154 – 0.123×Freq + 0.049×Emb. + 0.134×Cent. + 0.475×Bes. (12)

Where:

D is the damping ratio; Freq is the operating frequency (Hz); Sh is the shape of the foundation; Emb. is the embedment depth of the foundation; Sr is the degree of saturation %; Cent. is the point in the centerline under the foundation; Bes. is the point below and beside the foundation.

## 5 Conclusions

In this paper, soil characteristics of saturated clay subjected to harmonic vibration load are successfully investigated by the analytical solutions derived in frequency, displacement, and acceleration. This methodology can be the fundamental solution to finding the soil's damping ratio and shear modules. Finally, the main conclusions are observed.

1. The damping ratio increases with increased embedment depth because additional soil reaction on the sides of the embedded foundation has had a significant effect.
2. The increase in the embedment depth increases the natural frequency inside the soil.
3. The Young's and shear modulus increase with increasing operating frequency.
4. Generally, the damping ratio decreases for all cases when the frequency increases.
5. The damping ratio is a function of many factors, such as embedment depth, degree of saturation, shape of foundation, and operation frequency of the machine.

**Acknowledgment**

The authors acknowledge the financial support from the INTI IU Research Seeding Grant 2023: INTI-FEQS-1-06-2023. We also express our gratitude to the Civil Engineering Department, University of Technology, Baghdad, Iraq, for their assistance in acquiring data for the research.

## References

[1] Abdulrasool, A. S. 2021. Experimental Investigation of Damping of Saturated and Unsaturated Soil under Machine Foundation. PhD Thesis, University of Technology, Baghdad, Iraq.

[2] Brennan AJ, Thusyanthan NI, Madabhushi SPG .2005. Evaluation of shear modulus and damping in dynamic centrifuge tests. J Geotech Geoenviron Eng., ASCE, https://doi.org/10.1061/ (ASCE)0733-9410(1994)120:6(996).

[3] Idriss I.M., Dobry R. and Singh R.D. 1978. Nonlinear behavior of soft clays during cyclic loading conditions. Journal of the Geotechnical Engineering, ASCE, 104: 1427–1447.

[4] Chowdhury, I. and Dasgupta, S. 2009. Dynamics of Structure and Foundation – A Unified Approach. CRC Press-Balkema, London.

[5] Dobry, R., Vucetic, M. 1987. Dynamic Properties and Seismic Response of Soft Clay Deposits. Int Symp Geotech Eng Soft Soils, Ciudad México, 51–87.

[6] Kallioglou, P., Tika T., Koninis G., Papadopoulos S., and Pitilakis K. 2009. Shear modulus and damping ratio of organic soils. Geotechnical and Geological Engineering 27 (2): 217–235. https://doi.org/10.1007/s10706-008-9224-1.

[7] Dutta TT, Saride S, Jallu M. 2016. Effect of saturation on dynamic properties of compacted clay in a resonant column test. Geomechanics and Geoengineering; 12(3): p.p 181–90. https://doi.org/10.1080/17486025.2016.1208849.

[8] Ali, A. F., Fattah, M. Y., Ahmed, B. A., 2017. Behavior of Dry Medium and Loose Sand-foundation System acted upon by Impact Loads. Structural Engineering and Mechanics, Vol. 64, No. 6, pp. 703-721., Techno Press, Korea. DOI: https://doi.org/10.12989/sem.2017.64.6.703.

[9] Ali, A. F., Fattah, M. Y., Ahmed, B. A. 2018. Response of Circular Footing on Dry Dense Sand to Impact Load with Different Embedment Depths. Earthquakes and Structures, Vol. 14, No. 4, pp. 323-336, Techno Press, Korea. DOI: https://doi.org/10.12989/eas.2018.14.4.000.

[10] Amir-Faryar, B. , Aggour, M. S. and McCuen, R. H. 2017.Universal model forms for predicting the shear modulus and material damping of soils. Geomechanics and Geoengineering: an International Journal 12(1), 60–71.

[11] Abdulrasool, A. S., Fattah, M. Y. and Salim, N. M., 2020. Application of Energy Absorbing Layer to Soil-structure Interaction Analysis. IOP Conference Series Materials Science and Engineering 737:012094, Fourth International Conference on Buildings, Construction and Environmental Engineering – BCEE4, Istanbul - Turkey October 7 – 9, 2019, DOI: 10.1088/1757-899X/737/1/012094.

[12] Abdulrasool, A.S., Fattah, M. Y., Salim, N. M., 2021. Experimental Investigation for Dynamic Response of Saturated Clay under Machine Foundation. Lecture Notes in Civil Engineering, 2021, 112, pp. 365–374.

[13] Prakash, S. 1981. Soil Dynamics. McGraw-Hill New York.

[14] Fattah, M. Y., Salim, N. M., Al-Shammary, W. T. 2015. Effect of Embedment Depth on Response of Machine Foundation on Saturated Sand. Arabian Journal for Science and Engineering, Vol. 40, No. 11, pp. 3075–3098, DOI 10.1007/s13369-015-1793-8, Springer Publishing.

[15] Venkatramaiah, C., 2006. Geotechnical Engineering. New Age International (P) Ltd.

[16] Barkan, D.D. 1962. Dynamics of Bases and Foundations‖. McGraw-Hill Book Co., New York, USA.

[17] Prasad, B. B. and Director, F. 2011. Advanced Soil Dynamics and Earthquake Engineering. New Delhi.

[18] Saran, S. 1999. Soil Dynamics and Machine Foundations. Suneel Galgotia for Galgotia Publications

(P) Ltd, Ansari Road, Darya Ganj, New Delhi.
[19] Fattah, M. Y., Ali, A. F., Ahmed, B. A. 2018. Impact Induced Responses of Saturated and Dry Dense Sand. International Journal of Geotechnical Earthquake Engineering Volume 9, Issue 2, July-December 2018, International Journal of Geotechnical Earthquake Engineering Volume 9, Issue 2, July-December 2018, pp. 63-85. DOI: 10.4018/IJGEE.2018070105.44.